Dinuclear cobalt(III) and mixed valence trinuclear MnIII–MnII–MnIII complexes with a tripodal bridging…

Article *in* New Journal of Chemistry · May 2016

DOI: 10.1039/C5NJ03670D

7 authors, including:

E. Carolina Sañudo
University of Barcelona
113 PUBLICATIONS **2,798** CITATIONS
SEE PROFILE

Andrés Vega
Universidad Andrés Bello
113 PUBLICATIONS **812** CITATIONS
SEE PROFILE

Monica Soler
University of Chile
40 PUBLICATIONS **1,463** CITATIONS
SEE PROFILE

NJC

PAPER

Cite this: *New J. Chem.*, 2016, **40**, 6164

Dinuclear cobalt(III) and mixed valence trinuclear Mn^{III}–Mn^{II}–Mn^{III} complexes with a tripodal bridging pyridylaminophenol ligand†

Ruben Davila,[a] Nicolas Farias,[a] E. Carolina Sañudo,[b] Andrés Vega,[cd] Albert Escuer,[b] Mónica Soler*[a] and Jorge Manzur*[a]

Received (in Victoria, Australia) 23rd December 2015, Accepted 5th May 2016

DOI: 10.1039/c5nj03670d

www.rsc.org/njc

A dinuclear cobalt(II), $[Co_2(\kappa^4\text{-}O,O',N,N'\text{-}L)_2(\mu\text{-}O,O'\text{-}HCOO)](ClO_4)\cdot(C_2H_5)_2O$ (**1**) and a linear mixed valence trinuclear manganese, $[Mn_3(\kappa^4\text{-}O,O',N,N'\text{-}L)_2(\mu\text{-}CH_3O)_2(\mu\text{-}O,O'\text{-}CH_3COO)_2]\cdot 2(C_2H_5)_2O$ (**2**) complexes with the ligand *N*-(2-pyridyl-methyl)-*N*,*N*-bis-[2′-hydroxy-5′-methyl-benzyl]-amine (H_2L) are reported. For both complexes the ligand is present in the deprotonated form. The coordination sphere of the cobalt centres can be described as slightly distorted octahedral with two bridging *O*-phenoxo, one *N*-pyridine, one *N*-amine, one terminal *O*-phenoxo and one bridging *O*-formate donor atoms. Interestingly, the bridging formate resulted from the aerial oxidation of methanol. The manganese complex (**2**) has a linear mixed valence Mn^{III}–Mn^{II}–Mn^{III}, with the Mn^{II} and Mn^{III} centres bridged by alkoxo, carboxylate and phenoxo groups. Cyclic voltammetry studies show both metal and ligand centred redox processes consistent with the structure of the complexes. Complex (**2**) has an $S = 3/2$ ground state; magnetic susceptibility measurements indicate a weak antiferromagnetic interaction. The best fit of the magnetic susceptibility data as a function of temperature was obtained using a conventional trinuclear linear model [$H = -2J(S_1S_2 + S_1S_3)$] with $J = -0.79$ cm^{-1} and $g = 1.99$.

Introduction

Several areas of research have been devoted to the synthesis of new polynuclear metal complexes, where multiple metal ions are incorporated into a single molecular entity linked by bridging ligands. Due to their size and molecular properties such complexes have interesting potential applications.[1] One of these areas is molecular magnetism. Applications of these species as magnetic molecules or as precursors for molecular materials depend on their properties, that are based on the spin ground state values and the magnetic interactions between the metal ions.[2] Another area of interest is the development of new redox catalysts.[3] The activation and use of oxygen for the oxidation and functionalization of organic substrates are one of the most important reactions in chemistry. These oxidation reactions can be carried out using a wide range of catalysts. In particular, the search for polynuclear metal complexes for mimicking biologically active enzymes has generated a big family of new complexes. Some examples are the manganese polynuclear complexes which have been studied mainly due to the involvement of manganese in the photosynthetic water oxidation system.[4–13] Besides, oxygen activation by cobalt complexes bearing different ligands has been extensively investigated as chemical models of dioxygen-carrying proteins, such as hemoglobin and myoglobin,[14] and as active oxidants in the oxidation of organic substrates.[15]

The synthesis of polynuclear metal complexes is a self-assembly process which depends highly on the experimental conditions, where small changes may lead to completely different results.[16] During the last 20 years, the discovery of coordination cluster compounds has increased exponentially due to advances in single crystal X-ray crystallography, which has allowed the elucidation of the molecular structure of compounds with the increasing size and complexity.[1]

Pyridylaminophenols are interesting *O*,*N*-polydentate ligands, since they can produce different polymetallic complexes, depending on the synthetic conditions used.[17] Two trinuclear Mn^{III} complexes of the general formula $[Mn_3L_2(\mu\text{-}OH)(OAc)]ClO_4$ (H_3L = 1-[*N*-(2-pyridylmethyl),*N*-(2-hydroxybenzyl)amino]-3-[*N*′-(2-hydroxybenzyl), *N*′-(4-X-benzyl)amino]propan-2-ol; X = Me, H)

[a] *Deapartamento de Ciencia de los Materiales, Facultad de Ciencias Físicas y Matemáticas, Universidad de Chile, Santiago, Chile. E-mail: jmanzur@ing.uchile.cl, msoler@ing.uchile.cl*
[b] *Departament de Química Inorgánica, Universitat de Barcelona, Martí i Franqués 1-11, 08028-Barcelona, Spain*
[c] *Departamento de Ciencias Químicas, Facultad de Ciencias Exactas, Universidad Andres Bello, Viña del Mar, Valparaíso, Chile*
[d] *Centro para el Desarrollo de la Nanociencia y la Nanotecnología (CEDENNA), Santiago, Chile*

† Electronic supplementary information (ESI) available. CCDC 1443367 and 1443368. For ESI and crystallographic data in CIF or other electronic format see DOI: 10.1039/c5nj03670d

have been prepared and characterized by Ledesma *et al.*[18] In these compounds three Mn atoms occupy the vertices of a nearly isosceles triangle, and four bridges are seen in their structure: two alkoxo and one phenoxo bridges from the ligands and one hydroxo bridge. Hirotsu *et al.*[19] reported the synthesis and characterization of manganese complexes with a series of N_2O_2 ligands derived from bis-*N*,*N*-(2-hydroxybenzyl)-*N*′,*N*′-dimethylethylenediamine. Linear mixed valence trinuclear manganese complexes are reported. The Mn^{II} and Mn^{III} ions are bridged by alkoxo, carboxylate and phenoxo bridges. Gultneh *et al.*[20] reported the synthesis and characterization of the dinuclear Mn^{II}_2 complex $[Mn_2(LO)(OAc)_2]ClO_4$ with the pyridylaminophenol ligand LOH, 2,6-bis((bis(2-(2-pyridyl)ethyl)-amino)methyl)phenol. Using different related ligands, several dinuclear and trinuclear manganese complexes have been reported.[21–28] The isolation of a mixed-valence trinuclear manganese complex $Mn^{II}Mn^{III}_2(SALADHP)_2$ $(O_2CCH_3)_4$–$(CH_3OH)_2$ ($H_2SALADHP$ = 2-salicylidene-amino)-1,3-dihydroxy-2-methylpropane) potentially relevant to the photosynthetic oxygen-evolving complex has been reported by Li *et al.*[21] Four mixed valence trinuclear manganese complexes of general stoichiometry $Mn^{II}Mn^{II}_2L_2$(carboxylate) where, L is a tridentate salicylidene amino Schiff base ligand and X is a neutral monodentate donor, have been structurally characterized.[22] The synthesis and characterization of a valence trapped binuclear mixed-valence Mn(II,III) complex prepared from a new septadentate ligand, HL-Im = 2,6-bis[(bis-((1-methylimidazol-2-y1)methyl)amino) methyl]-4-methyl-phenol was reported by Buchanan *et al.*[23]

A few examples of cobalt complexes with ligands having mixed phenolate and pyridyl pendant groups have been reported in the literature. Acetate and perchlorate dinuclear metal complexes of Co(II), Cu(II) and Zn(II) with the polypodal ligand 2,6-bis[(2-hydroxybenzyl)(2-pyridylmethyl)aminomethyl]-4-methylphenol, have been reported by Martínez-Sánchez *et al.*[24] Binuclear cobalt(II) complexes, $[Co_2(bpmp)(CH_3COO)_2]ClO_4$ and $[Co_2(bpmp)(CH_3COO)](ClO_4)_2$ with the ligand 2, 6-bis[bis(2-pyridylmethyl) aminomethyl]-4-methylphenol (Hbpmp), were reported by Masatatsu Suzuki *et al.*[25] Interestingly, these complexes showed reversible oxygenation in several solvents. Frank B. Johansson *et al.*[26] reported a biphenol-based tetranucleating ligand, 2,2′,6,6′-tetrakis-(*N*,*N*-bis(2-pyridyl-methyl)aminomethyl)-4,4′-bi-phenolate (bpbp), and the corresponding homo and hetero tetranuclear complexes containing Zn, Fe, Cu and Co.

In earlier work, we have studied the copper coordination chemistry of a series of pyridyl-aminophenol ligands and mononuclear, dinuclear and trinuclear copper complexes were reported.[17,29] We herein report the synthesis and characterization of a dinuclear cobalt(III) and a mixed valence linear trinuclear manganese complexes with the ligand *N*-(2-pyridyl-methyl)-*N*,*N*-bis-[2′-hydroxy-5′-methyl-benzyl]-amine.

Experimental

Equipment

Elemental analysis was performed at the Elemental Analysis Service, Universidad Andres Bello, Chile. FT-IR spectra were recorded, using KBr pellets, on a Bruker Vector 22 equipment. ^{1}H-NMR spectra were recorded in $CDCl_3$ on a BrukerAMX-300 NMR spectrometer. Chemical shifts are reported as δ values downfield of an internal Me_4Si reference. Magnetic susceptibility measurements for (**1**) were carried out on polycrystalline samples, at the Servei de Magnetoquimica of the Universitat de Barcelona, using a Quantum Design SQUID MPMS-5 equipment working in the range of 2–300 K under external magnetic fields of 3000 G and 95 G. Cyclic voltammograms were obtained on a Bas CW50 potentiostat, using a platinum counter electrode, a Ag/AgCl (3 M KCl) reference electrode and a glassy carbon as the working electrode, and using 0.1 M tetrabutylammonium perchlorate as the supporting electrolyte, in acetonitrile solution (sample concentration = 0.001 M) at 100 mV s^{-1}. All potentials are given *versus* the ferrocene/ferrocinium$^+$ couple. Under the conditions used, the Fc/Fc$^+$ couple appears at $E_{1/2}$ = 445 mV (Δp = 70 mV).

X-Ray diffraction

Suitable single crystals of 0.25 × 0.22 × 0.10 mm^3 for (**1**) and 0.10 × 0.10 × 0.05 mm^3 for (**2**) were mounted on a glass fiber. Data collection was performed on a Bruker Smart Apex II system using MoKα radiation (λ = 0.710690 Å). Crystallographic data and refinement details are listed in Table 1. Data reduction was conducted using SAINT,[30] while the structure solution by direct methods, completion and refinement was conducted using SHELXL.[31] Multi-scan absorption corrections were applied using SADABS.[32] The hydrogen atom positions were calculated after each cycle of refinement using SHELXL, using a riding model for each structure. During the structure completion process by difference Fourier synthesis, it was clear that some ill defined electron density was present in the holes left by the molecules of (**2**). Since the structure completion until this point shows a complete and unequivocal charge balance, ruling out the possibility of having an anion, the density should correspond to the solvent. Efforts to model this remaining and no-assigned density as solvent molecules gave no meaningful result in terms of identification of the molecules and also in terms of a significant lowering of the *r*-index. Re-recording of the data set using a longer collection time or lowering the distance between frames (both limited by crystal decomposition) in at least three different crystals from different crystallization batch led to the same situation. This led us to trythe use PLATON SQUEEZE,[33] a well documented method used for modelling of unresolved electron density,[34] in order to deal with the solvent unassigned electron density. PLATON analysis shows two elongated voids into the unit cell, as depicted in the Fig. S1, ESI.† Thermogravimetric analysis shows a peak at *ca.* 55 C corresponding to a weight loss of 13%, which is consistent with the easy release of the crystallization solvent molecules by the solid (Fig. S2, ESI†). The poor quality of the refinement indexes is then attributable to solvent disorder. In spite of the use of SQUEEZE, the indices remain high. These do not preclude the discussion of the structure of complex (**2**).

Synthesis of the ligand

All materials used in this work were of reagent quality and were used without further purification. The ligand *N*-(2-pyridylmethyl)-*N*,*N*-bis-[2′-hydroxy-5′-methyl-benzyl]-amine, H_2L, was obtained by

Table 1 Crystal data and structure refinement details for $[Co_2(\kappa^4\text{-}O,O',N,N'\text{-}L)_2(\mu\text{-}O,O'\text{-}HCOO)]\text{-}(ClO_4)\cdot(C_2H_5)_2O$ (**1**) and $[Mn_3(\kappa^4\text{-}O,O',N,N'\text{-}L)_2\text{-}(\mu\text{-}CH_3O)_2(\mu\text{-}O,O'\text{-}CH_3COO)_2]\cdot 2(C_2H_5)_2O$ (**2**)

	(**1**)	(**2**)
FW/uma	1029.28	1186.06
Crystal system	Monoclinic	Triclinic
Space group	$P2_1/n$	$P\bar{1}$
a/Å	11.8421(4)	11.829(4)
b/Å	25.8186(10)	12.643(4)
c/Å	15.2975(6)	21.233(6)
α/°	90	78.054(13)
β/°	98.783(2)	89.491(13)
γ/°	90	64.271(11)
V/Å^3	4622.3	2787.1(14)
Z (Z')	4	2
δ/g cm^{-3}	1.479	1.220
μ/mm^{-1}	0.84	0.72
F000	1944	1062
θ range	θ_{min} = 1.9°, θ_{max} = 29.3°	θ_{min} = 1.8°, θ_{max} = 26.0°
hkl range	$h = -16 \rightarrow 17$	$h = -14 \rightarrow 14$
	$k = -35 \rightarrow 35$	$k = -15 \rightarrow 14$
	$l = -20 \rightarrow 20$	$l = -26 \rightarrow 26$
N_{tot}, N_{uniq} (R_{int}), N_{obs}	37 112, 12 000 (0.060), 8349	19 768, 10 747 (0.087), 7062
Refinement parameters	610 parameters (1 restrain)	605 (0 restrain)
GOF	1.10	1.050
R_1, wR_2 (obs)	0.0530, 0.1394	0.154, 0.376
R_1, wR_2 (all)	0.0895, 0.1754	0.189, 0.401
Max. and min $\Delta\rho$	Δ_{max} = 0.93, Δ_{min} = −1.12	Δ_{max} = 1.95, Δ_{min} = −1.26

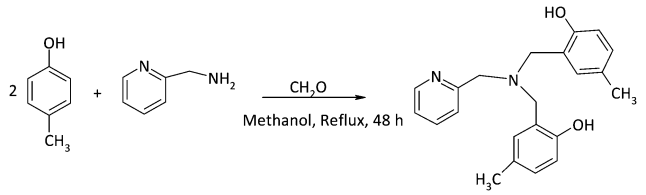

Scheme 1 Synthesis of the ligand *N*-(2-pyridylmethyl)-*N*,*N*-bis-[2′-hydroxy-5′-methyl-benzyl]-amine, H_2L.

the Mannich reaction of bis(2-pyridylmethyl) amine, paraformaldehyde and *p*-cresol (Scheme 1). To a suspension of p-formaldehyde (0.06 moles) in methanol (100 mL) 2-pyridylmethyl-amine (0.03 moles) and *p*-cresol (0.06 moles) were added. The reaction mixture was refluxed for 48 h, the solvent was removed under vacuum and the residue recrystallized from acetonitrile. Yield 50%. Anal. exp.% (calc. for $C_{23}H_{22}N_2O_2$): C: 76.7 (77.1), H: 6.0 (6.1), N: 7.6 (7.8)%.

^{1}HNMR ($CDCl_3$): δ 8.65 (1H, d, H_α-Py), 7.7 (1H, t, H_β-Py), 7.27 (1H, t, H_γ-Py), 7.12 (1H, d, H_δ-Py), 6.98 (2H, dd), 6.87 (2H, d) and 6.80 (2H, d, H-Ph), 3.89 (2H, s, CH_2-Py), 3.78 (4H, s, CH_2-Ph), 2.25 (6H, s, CH_3-Ph), 3.78 (4H, s, CH_2-Ph), 2.25 (6H, s, CH_3-Ph), 10.5 (2H, broad, OH).

Synthesis of complexes

$[Co_2(\kappa^4\text{-}O,O',N,N'\text{-}L)_2(\mu\text{-}O,O'\text{-}HCOO)](ClO_4)\cdot(C_2H_5)_2O$ (1). This complex was synthesized by the initial reaction of H_2L (97 mg, 0.27 mmol) with NaOMe (30 mg, 0.56 mmol) in methanol, and subsequent slow addition of a solution of $Co(ClO_4)_2\cdot 6H_2O$ (204 mg, 0.56 mmol) in MeOH. The reaction solution was stirred for an additional hour, and then left open until it crystallizes. To isolate single crystals, the solution was layered with ether. Yield 25%. Anal. exp.% (calc. for $C_{49}H_{55}ClCo_2N_4O_{11}$): C: 57.04 (57.13), H: 5.31(5.39), N: 5.26 (5.44); Co: 11.53 (11.45). IR (ν/cm^{-1}) 2883, 1610, 1570, 1485, 1452, 1360, 1284, 1269, 1119, 1087, 965, 940, 810, 757, 718, 670, 620, 560, 485, 440.

$[Mn_3(\kappa^4\text{-}O,O',N,N'\text{-}L)_2(\mu\text{-}CH_3O)_2(\mu\text{-}O,O'\text{-}CH_3COO)_2]\cdot 2(C_2H_5)_2O$ (2). This complex was synthesized by the reaction of H_2L (97 mg, 0.27 mmol) with NaOMe (30 mg, 0.56 mmol) in methanol, and subsequent slow addition of a solution of $Mn(OAc)_2\cdot 4H_2O$ (14 mg, 0.56 mmol) in MeOH. After an hour of stirring, the solution was left unperturbed until compound (**2**) crystallizes. Single crystals were obtained by layering the filtered solution with ether. Yield 30%. Anal. exp.% (calc. for $C_{58}H_{76}Mn_3N_4O_{12}$): C: 58.04 (58.69), H: 6.21(6.46), N: 4.96 (4.72); Mn: 14.2 (13.9). IR (ν/cm^{-1}) 2920, 2860, 1600, 1560, 1488, 1416, 1269, 1150, 1130, 1015, 965, 940, 820, 760, 718, 657, 624, 585, 510, 485, 417.

Results and discussion

The compounds $[Co_2(\kappa^4\text{-}O,O',N,N'\text{-}L)_2(\mu\text{-}O,O'\text{-}HCOO)]\ (ClO_4)\cdot(C_2H_5)_2O$ (**1**) and $[Mn_3L_2(CH_3O)_2(CH_3COO)_2]$ (**2**) were synthesized by a room temperature reaction of the diprotonated ligand *N*-(2-pyridylmethyl)-*N*,*N*-bis-[2′-hydroxy-5′-methyl-benzyl]-amine with the appropriate metal salt, cobalt perchlorate or manganese acetate, respectively. Single crystals of both complexes were isolated by layering the reaction mixture with ether.

Structural description

$[Co_2(\kappa^4\text{-}O,O',N,N'\text{-}L)_2(\mu\text{-}O,O'\text{-}HCOO)](ClO_4)\cdot(C_2H_5)_2O$ (1). Complex (**1**) corresponds to a Co^{III} dinuclear with two distorted edge-sharing slightly distorted octahedral sites. Each Co^{III} site display the deprotonated form of the *N*-(2-pyridylmethyl)-*N*,*N*-bis-[2′-hydroxy-5′-methyl-benzyl]amine molecule, acting as a

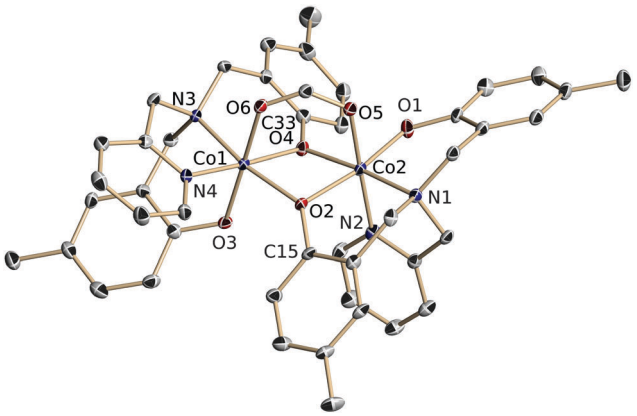

Fig. 1 Molecular structure of the $[Co_2(\kappa^4\text{-}O,O',N,N'\text{-L})_2(\mu\text{-}O,O'\text{-HCOO})]^+$ cation, at the 50% level of probability and partial atomic numbering scheme. The perchlorate counter anion, the solvating ethyl-ether and the hydrogen atoms have been omitted for clarity.

tetradentate ligand through two phenolate oxygen atoms, one aliphatic and one aromatic nitrogen amine atom. It is important to emphasize that these two phenolate oxygen atoms, belonging to each of the two arms of the ligands, displays a *cis* correlation for Co1 while a *trans* correlation is displayed for Co2. The two remaining positions on each cobalt site are occupied by a formate oxygen and a phenolate oxygen atoms from the neighbour cobalt site, as depicted in Fig. 1. Since no formate-containing molecule was used during the synthesis, it was probably formed through the aerial oxidation of methanol, catalysed by the cobalt complex. Oxidations of alcohols by molecular oxygen catalyzed by cobalt complexes have been reported in the literature.[35]

The $[Co_2(\kappa^4\text{-}O,O',N,N'\text{-L})_2(\mu\text{-}O,O'\text{-HCOO})]^+$ cation displays three covalent bridges of two different kind connecting each of the Co^{III} sites. One of them is a triatomic bridge defined by a formate anion, which connects each cobalt site with one of its oxygen atoms (see Fig. 1), in a *syn* mode. The other two bridges are monoatomic and are constituted by phenolate oxygen atoms. In this way, the distance between the Co^{III} sites inside the cation is 2.9587(6) Å. As a consequence of the presence of the formate anion connecting the apices of the two edge sharing octahedrons of the $[Co_2(\kappa^4\text{-}O,O',N,N'\text{-L})_2(\mu\text{-}O,O'\text{-HCOO})]^+$ cation, the respective equatorial planes are not coplanar, as normally occurs for Co_2O_2 connected dinuclear complexes. The dihedral angle between the least squares planes defined by the equatorial planes (Co1, O2, O4, N3, N4 and Co2, O2, O4, O1, N1) is 155.9(3)°. Selected bond distances and bond angles are given in Table 2.

$[Mn_3(\kappa^4\text{-}O,O',N,N'\text{-L})_2(\mu\text{-}CH_3O)_2(\mu\text{-}O,O'\text{-}CH_3COO)_2]\cdot 2(C_2H_5)_2O$ (2). The crystal structure of (2) is composed by two linear and crystallographically non-equivalent; although highly similar; trinuclear manganese units of formula $[Mn_3(\kappa^4\text{-}O,O',N,N'\text{-L})_2(\mu\text{-}CH_3O)_2(\mu\text{-}O,O'\text{-}CH_3COO)_2]$. In the following paragraphs, we will refer to them as **2-I** (Mn1/Mn2/Mn1^i) (Fig. 2) and **2-II** (Mn4/Mn3/Mn4^{ii}) (Fig. S3, ESI†).

The coordination geometry around each manganese centre would be well described as non-regular octahedrons. Since both units have a crystallographic inversion centre at the central manganese cation, their point symmetry is C_i. Each terminal manganese site displays a molecule of L^{2-} acting as a tetradentate ligand through two phenolate oxygen atoms, one aliphatic and one aromatic nitrogen amine atoms. The phenolate oxygen atoms display a *trans* correlation, as the coordination mode for Co2 in (1). Each terminal Mn centre displays three different covalent bridges connecting them to the central Mn^{II} site. The first of them is a triatomic bridge defined by an acetate anion in a *syn* mode. The second and the third bridges are monoatomic and are constituted by one phenolato and one methoxo oxygen atoms. Thus, the central manganese is coordinated octahedrally by six oxygen donors. The Mn2–O distances are 2.177 Å for Mn2–O (phenolato), 2.180 Å for Mn2–O(carboxylato) and 2.126 Å

Table 2 Selected bond distances (Å) and angles (°) for (1) and (2)

(1)			
Co2–O1	1.859(2)	Co2–N1	1.955(3)
Co1–O2	1.992(2)	Co2–N2	1.922(3)
Co1–O3	1.875(2)	Co1–N3	1.960(3)
Co1–O4	1.910(2)	Co1–N4	1.912(3)
Co2–O2	1.947(2)	Co2–O4	1.937(2)
Co2–O5	1.930(2)	Co1···Co2	2.9587(6)
Co2–O6	1.944(2)		
O3–Co1–O4	91.42(9)	N4–Co1–Co2	138.28(8)
O3–Co1–N4	92.41(10)	O1–Co2–N2	94.09(11)
O4–Co1–N4	176.15(10)	O1–Co2–O5	88.67(10)
O3–Co1–O6	175.84(10)	N2–Co2–O5	174.80(11)
O4–Co1–O6	92.12(9)	O1–Co2–O4	91.23(9)
N4–Co1–O6	84.04(10)	N2–Co2–O4	91.63(10)
O3–Co1–N3	93.95(10)	O5–Co2–O4	92.72(9)
O4–Co1–N3	93.93(10)	O1–Co2–O2	169.83(10)
N4–Co1–N3	86.18(11)	N2–Co2–O2	88.76(10)
O6–Co1–N3	87.99(10)	O5–Co2–O2	89.29(9)
O3–Co1–O2	91.83(9)	O4–Co2–O2	78.92(9)
O4–Co1–O2	78.44(9)	O1–Co2–N1	93.18(10)
N4–Co1–O2	101.06(10)	N2–Co2–N1	85.41(11)
O6–Co1–O2	86.73(9)	O5–Co2–N1	90.03(10)
N3–Co1–O2	170.54(9)	O4–Co2–N1	174.85(10)
O4–Co1–Co2	40.05(6)	O2–Co2–N1	96.77(10)
(2)			
Mn1–O1	1.869(8)	Mn2–O5^i	2.125(7)
Mn1–O5	1.886(8)	Mn2–O5	2.125(7)
Mn1–O2	1.952(7)	Mn2–O2	2.177(7)
Mn1–N2	2.114(9)	Mn2–O2^i	2.177(7)
Mn1–O7	2.191(8)	Mn2–O6^i	2.185(9)
Mn1–N1	2.279(9)	Mn2–O6	2.185(9)
Mn1···Mn2	3.1010(17)	Mn···Mn1^i	3.1010(17)
O1–Mn1–O5	93.2(3)	O5^i–Mn2–O5	180
O1–Mn1–O2	176.7(3)	O5^i–Mn2–O2	107.1(3)
O5–Mn1–O2	83.5(3)	O5–Mn2–O2	72.9(3)
O1–Mn1–N2	90.2(3)	O5^i–Mn2–O2^i	72.9(3)
O5–Mn1–N2	172.6(4)	O5–Mn2–O2^i	107.1(3)
O2–Mn1–N2	93.1(3)	O2–Mn2–O2^i	180
O1–Mn1–O7	92.3(3)	O5^i–Mn2–O6^i	89.0(3)
O5–Mn1–O7	96.8(4)	O5–Mn2–O6^i	91.0(3)
O2–Mn1–O7	88.0(3)	O2–Mn2–O6^i	95.3(19)
N2–Mn1–O7	89.6(3)	O2^i–Mn2–O6^i	84.8(3)
O1–Mn1–N1	97.8(3)	O5^i–Mn2–O6	91.0(3)
O5–Mn1–N1	95.2(4)	O5–Mn2–O6	89.0 (3)
O2–Mn1–N1	82.7(3)	O2–Mn2–O6	84.8(7)
N2–Mn1–N1	77.7(4)	O2^i–Mn2–O6	95.2(3)
O7–Mn1–N1	163.8(3)	O6^i–Mn2–O6	180
Mn1–O2–Mn2	97.15(19)	Mn1–O5–Mn2	101.1(3)

Symmetry codes: (i) $-x+1, -y+2, -z+1$; (ii) $-x+1, -y+1, -z$.

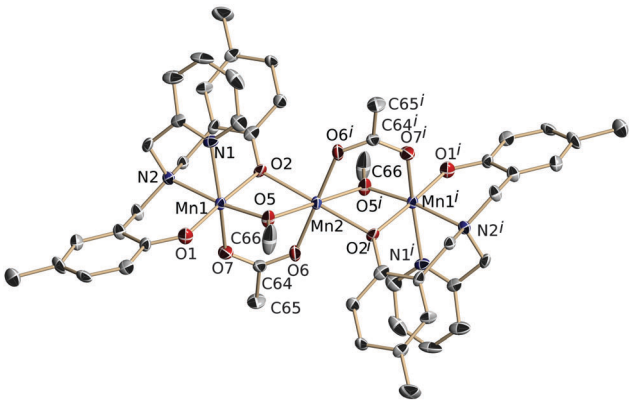

Fig. 2 Molecular structure of one (**2-I**) of the two non-equivalent trinuclear complex units $[Mn_3(\kappa^4\text{-}O,O',N,N'\text{-}L)_2(\mu\text{-}CH_3O)_2(\mu\text{-}O,O'\text{-}CH_3COO)_2]$ contained within the crystal structure of **2**. Displacement ellipsoids are drawn at the 50% level of probability and partial atomic numbering scheme is included. The hydrogen atoms have been omitted for clarity. The molecular structure of the second trinuclear unit (**2-II**) is shown in Fig. S3 (ESI†).

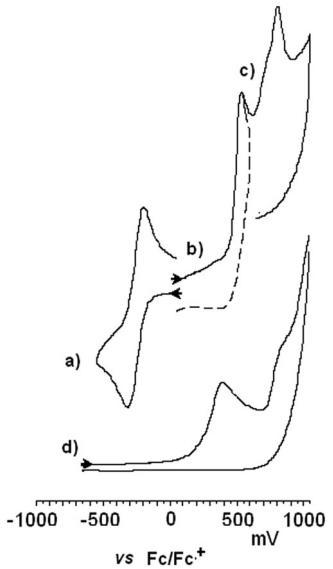

Fig. 3 Cyclic voltammogram of 0.001 M (**1**) in acetonitrile. Rate = 100 mV s^{-1}.

for Mn2–O(methoxo). These values are typical for those between the manganese(II) ion and the oxygen donors. On the other hand, the bond distances of the two terminal manganese centres are in the range expected for manganese(III): the Mn1–O(phenolato) distances are 1.865 Å and 1.954 Å for Mn1–O1 and Mn–O2 respectively, while the Mn1–O5(methoxo) distance is 1.890 Å, clearly shorter than the Mn2–O distances. Besides, the terminal Mn ions show a Jahn–Teller elongation axis along the N1–Mn1–O7 direction, as expected for high-spin Mn^{III} (d^4) in the near-octahedral geometry. Based on the above observations, the oxidation state of the central Mn2 is assigned to Mn^{II}, and those of the terminal Mn1 and Mn1′ centres are assigned to Mn^{III}.[21] The assignments of the oxidation states were confirmed by a bond valence sum (BVS) calculations.[36] BVS analysis has been used to verify oxidation states in metalloenzymes and superconductors, as well as many coordination complexes.[37] The bond valence sums resulted 3.00 for Mn1 and Mn1′ and 2.04 for Mn2 (Table S1, ESI†).

The distances between the Mn^{II} and the Mn^{III} centres in each unit are 3.1011(12) Å (**2-I**) and 3.1114(13) Å (**2-II**). As observed for (**1**), the presence of the *syn*-carboxylate anion, connecting the apices of the two consecutive edge sharing octahedrons, forces their equatorial planes not to be coplanar. The dihedral angle between the least squares planes defined by the equatorial planes (Mn1, O1, O5, O2, N2 and Mn2, O5, O2, $O2^i$, $O5^i$) is 19.7(4)° for **2-I** and 21.4(4)° for **2-II** (Mn4, O4, O10, O3, N4 and Mn3, O3, O10, $O3^{ii}$, $O10^{ii}$). Table 2 and Table S2 (ESI†) show a summary of interatomic distances and angles for **2-I** and **2-II**, respectively.

Electrochemistry

The electrochemistry of both complexes was studied by cyclic voltammetry in acetonitrile as solvent. Fig. 3 and 4 show the cyclic voltammograms for complexes (**1**) and (**2**) in the potential range of −1000 to 1000 mV (*vs.* Fc/Fc^+). For the dinuclear cobalt

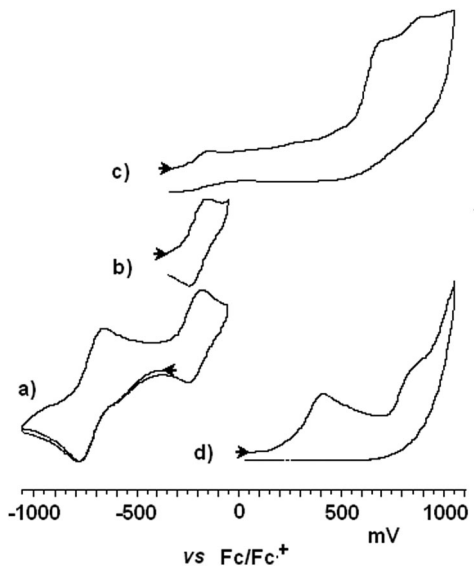

Fig. 4 Cyclic voltammogram of 0.001 M (**2**) in acetonitrile. Rate = 100 mV s^{-1}.

complex, a cathodic scan shows a quasi-reversible redox couple at $E_{1/2}$ = −352 mV (Δp = 115 mV) that can be ascribed to the metal centered $Co^{III}{}_2/Co^{II}{}_2$ redox process (Fig. 3a). The scanning towards anodic potentials shows an irreversible signal at E_p = 530 mV (Fig. 3b) and a second one at 880 mV (Fig. 3c). Both signals can be assigned to the oxidation of the phenoxo group to phenoxyl.[38] The voltammogram of the free ligand shows an irreversible anodic signal at 400 mV and a second one at 880 mV corresponding to the consecutive oxidation of the two phenol groups in the ligand (Fig. 3d). Starting at −300 mV, the manganese complex display a quasi-reversible cathodic signal at $E_{1/2}$ = −705 mV (Δp = 90 mV) assigned to the reduction of the two terminal manganese(III) ions (Fig. 4a). Scanning the anodic potentials, a first reversible signal is observed at $E_{1/2}$ = −200 mV

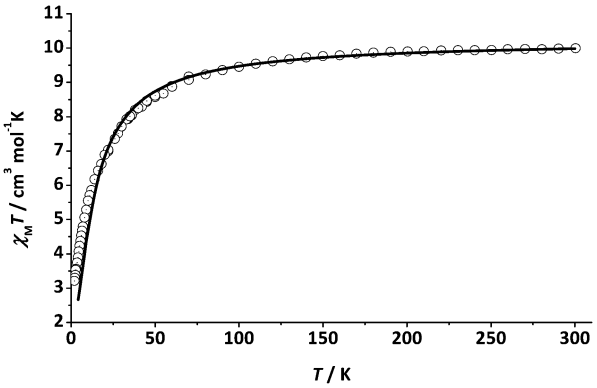

Fig. 5 Plot of the $\chi_M T$ product *vs.* T for (**2**). The solid line shows the best fit of the data.

(Δp = 70 mV) assigned to the oxidation of the central Mn^{II} ion (Fig. 4b). Continuing the anodic scan, two irreversible signals at 690 and 880 mV are seen (Fig. 4c); these redox processes may be assigned to ligand centred processes. Other metal complexes with ligands containing phenol groups show phenoxo–phenoxyl oxidations at similar potentials.[39–42]

Magnetic studies for (2)

Fig. 5 shows the magnetic susceptibility data as a function of temperature. The $\chi_M T$ value is almost constant and equal to 10 cm^3 mol^{-1} K until *ca.* 50 K. This value corresponds to the expected value for two Mn^{III} and one Mn^{II} isolated ions. At lower temperature it decreases quickly reaching a value of 3.20 cm^3 mol^{-1} K and tending to the value of 1.875 cm^3 mol^{-1} K expected for the fundamental S = 3/2 state.

The fit of the susceptibility data was done using the linear trinuclear model,

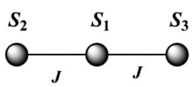

with $H = -2J(S_1S_2 + S_1S_3)$.

Because of the large distance between the terminal Mn^{III} ions (~6.2 Å) this interaction can be excluded and, therefore, the major exchange interaction is expected between the terminal Mn^{III} and the central Mn^{II}. The fit of the susceptibility data was done isotopically since it is satisfactory to explain the experimental results.

Furthermore, the measurements at two different magnetic fields (3000 G and 95 G) are identical, indicating a null anisotropy for the fundamental state. The best fit of the magnetic susceptibility data, as a function of temperature, was obtained with J = −0.79 cm^{-1} and g = 1.99.

Conclusions

We have synthesized and structurally characterized two new complexes with the tripodal *N*-(2-pyridyl-methyl)-*N*,*N*-bis-[2′-hydroxy-5′-methyl-benzyl]-amine, one Co^{III} dinuclear and a linear mixed valence Mn^{III}–Mn^{II}–Mn^{III} trinuclear complexes. The deprotonated ligand acts as a bridging tetradentate N_2O_2 ligand. The manganese complex shows an overall weak antiferromagnetic interaction between the metal centres. The bridging formate group observed in the cobalt complex resulted from the aerial oxidation of methanol, catalyzed by the cobalt complex. The cyclic voltammetric behaviour is consistent with the structure of the complexes.

The reported work shows the versatility of pyridylaminophenol ligands in the coordination chemistry of metal ions.

Acknowledgements

Financial support from project FONDECYT 1120109 is gratefully acknowledged. RD and MS thank Anillo project Act 1117. ECS acknowledges financial support from Spanish Ministry of Economy and Competitiveness project No CTQ2012-32247.

References

1 J. Fielden and L. Cronin, *Coordination Clusters Encyclopaedia of Supramolecular Chemistry*, 2005, pp. 1–10.
2 D. D. Willett, D. Gatteschi and O. Kahn, *Magneto-Structural Correlations in Exchanged Coupled Systems*, NATO-ASI Series, Reidel, Amsterdam, 1985.
3 R. A. Sheldon and J. A. Kochi, *Metal-catalyzed oxidations of organic compounds*, Academic Press, N.Y., 1981.
4 C. S. Mullins and V. L. Pecoraro, *Coord. Chem. Rev.*, 2008, **252**, 416–443.
5 E. A. Karlsson, B.-L. Lee, T. Åkermark, E. V. Johnston, M. D. Kärkäs, J. Sun, Ő. Hansson, J.-E. Bäckvall and B. Åkermark, *Angew. Chem., Int. Ed.*, 2011, **50**, 11715–11718.
6 K. J. Young, M. K. Takase and G. W. Brudvig, *Inorg. Chem.*, 2013, **52**, 7615–7622.
7 Y. Gao, T. Åkermark, J. Liu, L. Sun and B. Åkermark, *J. Am. Chem. Soc.*, 2009, **131**, 8726–8727.
8 P. Kurz, *Dalton Trans.*, 2009, 6103–6108.
9 E. A. Karlsson, B.-L. Lee, R.-Z. Liao, T. Åkermark, M. D. Kärkäs, V. Saavedra Becerril, P. E. M. Siegbahn, X. Zou, M. Abrahamsson and B. Åkermark, *ChemPlusChem*, 2014, **79**, 936–950.
10 J. S. Kanady, P.-H. Lin, K. M. Carsch, R. J. Nielsen, M. K. Takase, W. A. Goddard III and T. Agapie, *J. Am. Chem. Soc.*, 2014, **136**, 14373–14376.
11 C. Zhang, C. Chen, H. Dong, J.-R. Shen, H. Dau and J. Zhao, *Science*, 2015, **348**, 690–693.
12 L. Hammarström, *Curr. Opin. Chem. Biol.*, 2003, **7**, 666–673.
13 W. A. A. Arafa, M. D. Kärkäs, B.-L. Lee, T. Åkermark, R.-Z. Liao, H.-M. Berends, J. Messinger, P. E. M. Siegbahn and B. Åkermark, *Phys. Chem. Chem. Phys.*, 2014, **16**, 11950–11964.
14 S. Hikichi, M. Akita and Y. Moro-oka, *Coord. Chem. Rev.*, 2000, **198**, 61–87.
15 C. L. Bailey and R. S. Drago, *Coord. Chem. Rev.*, 1987, **79**, 321–332, and references therein.
16 B. Pignataro, *New strategies in Chemical Synthesis and Catalysis*, Wiley-VCH, 2012.

17 J. Manzur, H. Mora, A. Vega, E. Spodine, D. Venegas-Yazigi, M. T. Garland, M. S. El Fallah and A. Escuer, *Inorg. Chem.*, 2007, **46**, 6924–6932.
18 G. N. Ledesma, E. Anxolabéhère-Mallart, E. Rivière, S. Mallet-Ladeira, C. Hureau and S. R. Signorella, *Inorg. Chem.*, 2014, **53**, 2545–2553.
19 M. Hirotsu, M. Kojima and Y. Yoshikawa, *Bull. Chem. Soc. Jpn.*, 1997, 647–657.
20 Y. Gultneh, A. Farooq, S. Liu, K. D. Karlin and J. Zubieta, *Inorg. Chem.*, 1992, **31**, 3607–3611.
21 X. Li, D. P. Kessissoglou, M. L. Kirk, C. J. Bender and V. L. Pecoraro, *Inorg. Chem. Commun.*, 1988, **27**, 1–3.
22 D. P. Kessissoglou, J. Martin, L. Kirk, M. S. Lah, X. Li, C. Raptopoulou, W. E. Hatfield and V. L. Pecoraro, *Inorg. Chem.*, 1992, **32**, 5424–5432.
23 R. M. Buchanan, K. J. Oberhausen and J. F. Richardson, *Inorg. Chem.*, 1988, **27**, 971–973.
24 J. Martínez-Sánchez, R. Bastida, A. Macías, H. Adams, D. E. Fenton, P. Pérez-Lourido and L. Valencia, *Polyhedron*, 2010, **29**, 2651–2656.
25 M. Suzuki, H. Kanatomi and I. Murase, *Chem. Lett.*, 1981, 1745–1748.
26 F. B. Johansson, A. D. Bond and C. J. McKenzie, *Inorg. Chem.*, 2007, **46**, 2224–2236.
27 Z. J. Zhong and X.-Z. You, *Polyhedron*, 1994, **13**, 2157–2161.
28 V. Tangoulis, D. A. Malamatari, K. Soulti, V. Stergiou, C. P. Raptopoulou, A. Terzis, T. A. Kabanos and D. P. Kessissoglou, *Inorg. Chem.*, 1996, **35**, 4974–4983.
29 J. Manzur, H. Mora, D. Venegas-Yazigi, M. A. Novak, J. Sabino, V. Paredes-García and E. Spodine, *Inorg. Chem.*, 2009, **48**, 8845–8855.
30 *SAINTPLUS V6.22*, Bruker AXS Inc., Madison, WI, USA, 2000.
31 G. Sheldrick, *Acta Crystallogr.*, 2015, **C71**, 3–8.
32 *SADABS V2.05*, Bruker AXS Inc., Madison, WI, USA, 2001.
33 A. L. Spek, *J. Appl. Crystallogr.*, 2003, **36**, 7.
34 P. Van Der Sluis and A. L. Spek, *Acta Crystallogr.*, 1990, **A4**, 194.
35 M. S. Vad, A. Nielsen, A. Lennartson, A. D. Bond, J. E. McGrady and C. J. McKenzie, *Dalton Trans.*, 2011, 10698–10707.
36 (*a*) I. D. Brown and K. K. Wu, *Acta Crystallogr.*, 1976, **B32**, 1957; (*b*) R. M. Wood and G. J. Palenik, *Inorg. Chem.*, 1998, **37**, 4149–4151; (*c*) I. D. Brown and D. Altermatt, *Acta Crystallogr.*, 1985, **B41**, 244–247.
37 (*a*) I. D. Brown, *J. Solid State Chem.*, 1989, **82**, 122–131; (*b*) W. Liu and H. H. Throp, *Inorg. Chem.*, 1993, **32**, 4102–4105; (*c*) M. Soler, W. Wernsdorfer, K. A. Abboud, J. C. Huffman, E. R. Davidson, D. N. Hendrickson and G. Christou, *J. Am. Chem. Soc.*, 2003, **125**, 3576–3588.
38 M. M. Allard, F. R. Xavier, M. J. Heeg, H. B. Schlegel and C. N. Verani, *Eur. J. Inorg. Chem.*, 2012, 4622–4631.
39 C. Imbert, H. P. Hratchian, M. Lanznaster, M. J. Heeg, L. M. Hryhorczuk, B. R. McGarvey, H. B. Schlegel and C. N. Verani, *Inorg. Chem.*, 2005, **44**, 7414–7422.
40 M. M. Allard, J. A. Sonk, M. J. Heeg, B. R. McGarvey, H. B. Schlegel and C. N. Verani, *Angew. Chem., Int. Ed.*, 2012, **51**, 3178–3182.
41 U. K. Das, J. Bobak, C. Fowler, S. E. Hann, C. F. Petten, L. N. Dawe, A. Decken, F. M. Kerton and C. M. Kozak, *Dalton Trans.*, 2010, **39**, 5462–5477.
42 L. Chiang, L. E. N. Allan, J. Alcantara, M. C. P. Wang, T. Storr and M. P. Shaver, *Dalton Trans.*, 2014, **43**, 4295–4304.

